Magnon-Phonon Coupling in Metallic Films

R. WEBER

Lincoln Laboratory, Massachusetts Institute of Technology, Lexington, Massachusetts 02173*

(Received 27 November 1967)

The method of standing spin-wave resonance, which sensitively detects periodic changes in the transverse magnetization through the film thickness, has been used to study magnetoelastic coupling in several metallic films. The effect was recorded as a function of $\Delta\bar{H}_p$, the deviation of the magnetic field for resonance of the pth spin-wave mode in the presence of magnetoelastic coupling from the magnetic field for resonance of the same mode in the absence of coupling. The film compositions varied from the 81% Ni–19% Fe nonmagnetostrictive alloy to a 65% Ni–35% Fe alloy. The film thicknesses were of the order of 6000 Å. The frequency range of the experiment was 57 to 62 GHz. A calculation which combined the strain-wave equations with the equations of motion for the transverse magnetization m allowed for the solution of m as a product of a complex susceptibility χ and the magnitude of the cavity-produced rf magnetic field. In the calculation, trigonometric solutions were used for m and for the strain. For the sake of simplicity, the boundary conditions were taken to be $m=0$ (spin pinning) and zero stress at the film surfaces. Reχ described the dispersion, and was solved for $\Delta\bar{H}_p$. The presence of a phonon relaxation time was crucial in that it kept $\Delta\bar{H}_p$ finite. In fitting the theoretical $\Delta\bar{H}_p$ to the experimental data, values were obtained for the speed of transverse phonons ($\approx 3\times10^5$ cm/sec) in the film at the microwave frequency, for the magnitude of the magnetoelastic coupling constant ($\approx 6\times10^7$ erg/cm^3) at 77°K, and for the phenomenological phonon relaxation time ($\approx 1\times10^{-10}$ sec). The comparison of the calculated $\Delta\bar{H}_p$ with the data showed excellent agreement in the region near the crossover point. The agreement was less satisfactory away from the crossover point. Examination of $|\,\mathrm{Im}\chi\,|$, which is proportional to the power absorbed in the film, explains the qualitative behavior of the resonances in the crossover region, again indicating the important role played by the phonon relaxation time in the explanation of the effect of magnetoelastic coupling in metallic films.

INTRODUCTION

In a theoretical treatment of the magnetoelastic coupling of spin waves (magnons) and elastic waves (phonons) in a ferromagnetic crystal[1] it has been shown that the strength of the coupling is a maximum when conditions are such that spin waves and elastic waves of the same frequency have the same wave number; and that away from this resonance condition, the strength of the interaction decreases as the wave-vector difference between the magnons and the phonons increases. In this "crossover" region, where the coupling is greatest, the normal modes of the system are no longer either purely magnetic or purely elastic in nature, but are admixtures of both properties. The dispersion of these magnetoelastic modes differs from that of either the purely elastic or purely magnetic modes which would exist in the absence of coupling. This difference is most pronounced in the crossover region. It is to be expected that the dispersion of just the magnetic part of a magnetoelastic mode should reflect the dispersion of the combined mode. If so, then the measurement of this dispersion in a ferromagnetic metal over ranges of frequency and wave vector, including the crossover region, will yield information about magnon-phonon coupling in that metal. Since deviations from the usual quadratic behavior of spin waves in magnetic materials (because of zone effects) have been studied with accuracy by the method of spin-wave resonance in the past,[2] similar techniques have been used to observe the magnon-phonon interaction in suitable metallic, magnetic film samples.

EXPERIMENTAL CONSIDERATIONS

Experimental considerations called for the use of microwave frequencies of the order of 60 GHz and film thicknesses of the order of 6000 Å. These values ensured that crossover would occur among clearly defined, closely spaced allowed spin-wave resonance peaks.

Several nickel-iron films were selected for use on the basis that they were pure alloys, that their measured magnetizations ($4\pi M_s$) and g values agree with their bulk values, and that they exhibit many resolvable resonance peaks. Included in the selection was the nonmagnetostrictive 81% Ni–19% Fe alloy. This film composition was used as a test sample since it should exhibit no magnetoelastic coupling. The first five columns of Table I list the sample specifications.

In that the effect of magnon-phonon coupling was to be observed as magnetic field deviations of the spin-wave resonances from the spin-wave dispersion relation in the absence of such coupling, detailed measurements were made of the complete spin-wave spectra of the selected films at 298, 77.3, and 4.2°K. Small deviations, attributable to magnon-phonon coupling, were observed in several films at 4.2 and at 77.3°K. These deviations, extending over very limited ranges of the allowed spin-wave wave vectors, were not observable at 298°K. Since the deviations were unchanged at the lower temperatures, the coupling data were taken at 77.3°K. The room-temperature data were useful in establishing the reference dispersion (i.e., the dispersion in the

* Operated with support from the U.S. Air Force.

[1] C. Kittel, Phys. Rev. 110, 836 (1958).

[2] R. Weber and P. E. Tannenwald, Phys. Rev. 140, A498 (1965).

TABLE I. Sample specifications and experimental results for three nickel-iron films. $T=77.3°K$.

Sample	Composition Ni–Fe ±1	Thickness (Å) ±60	$4\pi M_s$ (kOe) ±0.03	g ±0.02	A (10^{-6} erg/cm) ±0.03	f_c (GHz)	p_c (corresp. to f_c)	c_t (10^5 cm/sec) ±0.03	b_2 (10^7 erg/cm^3) a	τ_s (10^{-10} sec) a
1	60–40	6920	14.96	2.14	1.20	58.25	26	3.10	6.74	0.76
2	70–30	6170	13.60	2.14	1.12	57.77	23	3.10	6.51	0.93
3	81–19	5040	10.90	2.08	0.91	...	...	...	...	...

[a] The intrinsic value of τ_s may differ from this value (see text). This would modify the b_2 value (Ref. 9).

absence of magnon-phonon coupling) for each film. The dispersive behaviors were all closely quadratic up to the higher-order modes, where the negative quartic term[2] became measurable. From the quadratic portions of the spectra, the exchange stiffness constants A were determined for the three selected films (Table I, Column 6).

The resonance expression for the discrete standing-wave modes excited by a microwave magnetic field in the plane of a thin film in the geometry of ferromagnetic resonance is given by

$$\omega=\gamma(H-4\pi M_s)+\gamma(2A/M_s)(\pi^2/L^2)p^2, \qquad (1)$$

where ω is the microwave frequency, γ is the gyromagnetic ratio, H is the applied dc magnetic field (perpendicular to the plane of the film), $4\pi M_s$ is the saturation magnetization, L is the film thickness, and p is the assigned mode number. p is related to k_p, the spin-wave wave vector for the pth mode, through the selection rule for thin films: $p=(L/\pi)k_p$. For a given film, the allowed k_p and their spacing in a magnetic field are determined by the film thickness. In the usual spin-wave resonance experiment only odd modes (p, an odd integer) are excited. In the present work, where the film thickness and the electromagnetic skin depth are comparable, even-numbered modes are also excited. The presence of these modes, less strongly excited than the odd modes, increases the experimental accuracy by supplying more data points.

The dispersion for transverse phonons is given by

$$\omega=c_t k_s, \qquad (2)$$

where c_t is the speed of transverse phonons propagating perpendicular to the plane of the film (i.e., along the film normal) and k_s is the phonon wave vector. $k_s=2\pi/\lambda_s$, where λ_s is the phonon wavelength.

In the crossover region for constant ω, $k_s\approx k_p$. In the elastic case, each ω-value determines a unique phonon wave vector, as given by Eq. (2). There is no magnetic field dependence. In the case of spin waves, for each ω, a given k value can be "tuned in" by the dc magnetic field, as given by Eq. (1). Therefore, in order to locate and to sample the crossover region in detail for each film sample, the microwave frequency ω was allowed to be an experimental variable. It was possible to vary the frequency in 0.20-GHz steps from 55.00 to 62.40 GHz. The spin-wave resonance spectrum was examined in detail for each ω in the usual manner, whereby the allowed spin-wave resonances are selectively excited as a function of the perpendicular dc magnetic field. This examination showed that the previously observed small deviations from the predominantly quadratic dispersive background were reproducible and predictable as a function of frequency and that they occurred for values of ω and k which were in approximate agreement with calculated values. A convenient parameter, at this point, is $\Delta\bar{H}_p$, which is defined as the difference between the magnetic field for resonance of the pth mode in the presence of magnetoelastic coupling and that field which would be required for resonance of the same mode in the absence of coupling. $\bar{H}_p$ is the dc magnetic field separation between the uniform mode and the pth magnetic wave mode. Within the crossover region, the fields which would be required for resonance were determined by both the room-temperature data and by an interpolative procedure using ranges of wave vector both above and below the crossover region (using the 77°K data).

Figures 1 and 2 show the data in terms of $\Delta\bar{H}$ plotted against the microwave frequency ω for the two magnetostrictive samples. Sample No. 3 (the non-magnetostrictive composition) presented no meas-

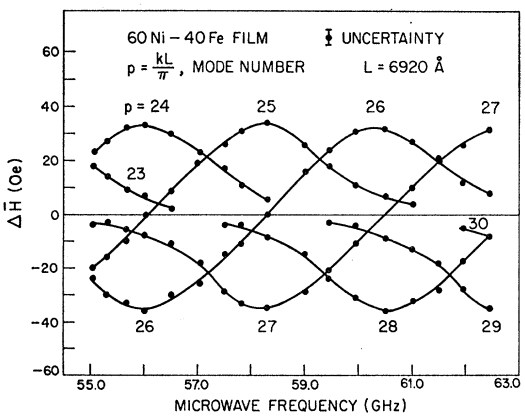

FIG. 1. Experimental data for sample 1. $\Delta\bar{H}$ is defined as the deviation in the magnetic field for resonance of a spin-wave mode in the presence of magnon-phonon coupling from the field for resonance of the same mode in the absence of such coupling. $T=77.3°K$.

urable deviations of the type of interest (i.e., $\Delta\bar{H}=0$). Since the frequency was variable, $\Delta\bar{H}_p$ has been treated as a continuous variable in these figures.

The symmetry of the data curves for the individual mode numbers suggests that it is reasonable to assign to each mode a microwave crossover frequency determined by the point of intersection of the $\Delta\bar{H}$ curve for that mode with the $\Delta\bar{H}=0$ axis. With this assignment, the crossover frequency f_c for the $p=26$ mode of sample 1 was 58.25 GHz; while for the $p=23$ mode of sample 2, f_c was 57.77 GHz. Note that points on the $\Delta\bar{H}=0$ axis correspond to resonances in the absence of magnetoelastic coupling.

Over the frequency range of the experiment, the shape of the curves of the separate modes (Figs. 1 and 2) are identical. This fact allowed for the composite constructions of the data, as presented in Figs. 3 and 4.

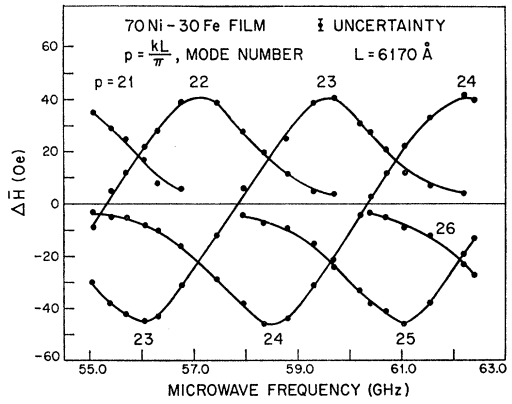

FIG. 2. Experimental data for sample 2. $\Delta\bar{H}$ is defined as for Fig. 1. $T=77.3$°K. For the nonmagnetostrictive sample 3, $\Delta\bar{H}=0$ over the appropriate frequency range.

DESCRIPTION OF ANALYSIS

A brief description of the analysis of the data begins with the equations of motion for small amplitudes for the magnetization and for the elastic displacement, as given in the literature.[1,3–5] In the present work, both phonon and magnon damping terms are added to the equations. Propagation in the direction of the dc magnetic field along the film normal (z direction), with no variation in the x and y direction, is considered. Further, if elastic isotropy is assumed, and if complex notation is introduced, the rather complicated system of coupled linear differential equations can be reduced to two coupled complex equations,

$$\ddot{R}+\frac{2}{\tau_s}\dot{R}-c_t^2\frac{\partial^2}{\partial z^2}R=\frac{b_2}{\rho M_s}\frac{\partial}{\partial z}m \qquad (3)$$

[3] E. Schlömann, J. Appl. Phys. **31**, 1647 (1960).
[4] W. Strauss, Proc. IEEE **53**, 1485 (1965).
[5] V. A. Ignatchenko and E. V. Kuz'min, Zh. Eksperim. i Teor. Fiz. **49**, 787 (1965) [English transl.: Soviet Phys.—JETP **22**, 547 (1966)].

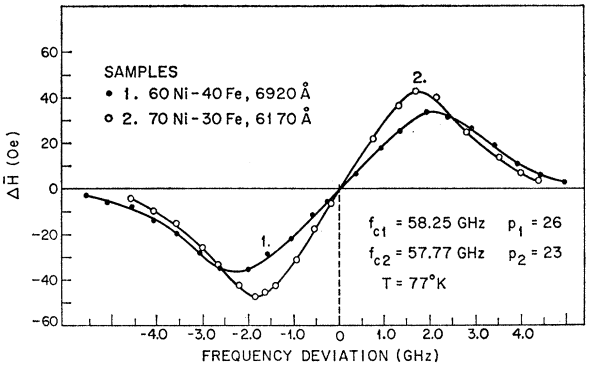

FIG. 3. Composite experimental data constructed from Figs. 1 and 2. $\Delta\bar{H}$ is plotted as a function of the frequency deviation around the assigned crossover frequencies for samples 1 and 2 (as discussed in the text). Each curve corresponds to a specific magnetic mode, as given by the appropriate mode numbers.

and

$$\dot{m}=i\gamma\left[\left(H+i\frac{1}{\gamma\tau_m}\right)m-\frac{2A}{M}\frac{\partial^2}{\partial z^2}m+b_2\frac{\partial}{\partial z}R-M_s h\right]. \qquad (4)$$

In Eqs. (3) and (4), R ($R=R_x+iR_y$) represents the transverse displacement of a point in the solid from its original position in the unstrained solid, τ_s is a phenomenological phonon relaxation time, c_t is the speed of transverse phonons in the film material (it is demonstrable that, to the first order, only transverse phonons couple appreciably with the z-directed magnons), ρ is the mass density, b_2 is the magnetoelastic coupling constant, m ($m=m_x+im_y$) is the transverse component of the magnetic moment, h is the transverse microwave magnetic field supplied by the cavity, H is the demagnitized dc magnetic field, τ_m is a phenomenological spin-wave relaxation time, A is the exchange stiffness constant, and M_s is the saturation magnetization.

The idea that the phonon and magnon relaxation

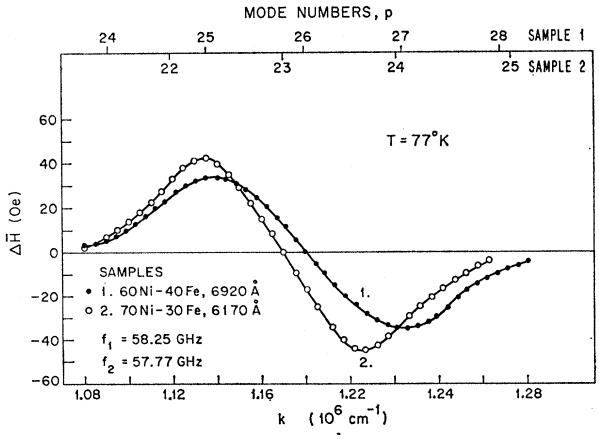

FIG. 4. A construction of the experimental data of Figs. 1 and 2 showing $\Delta\bar{H}$ versus the wave vector k. The microwave frequency was constant at the assigned crossover frequency for each sample (as discussed in the text).

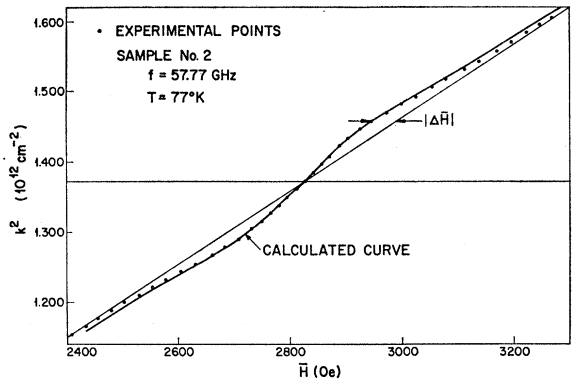

FIG. 5. Comparison of the experimental data with a derived expression for $\Delta\bar{H}$ [Eq. (5) in the text]. $\bar{H}$ is the magnetic field separation of a point in the spin-wave spectrum from the field for resonance of the uniform mode at constant microwave frequency. The light, sloping line represents the dispersion law obeyed in the absence of magnon-phonon coupling. The data points were taken from Fig. 4. The smooth curve through the points is the fit of Eq. (5) to the data.

parameters can be separated *even* in the crossover region is implicit in these equations. If the interaction is not too strong, such a concept is probably valid.[1]

The method of spin-wave resonance detects periodic changes in the net transverse magnetic moment m through the film thickness. Thus, the solutions of Eqs. (3) and (4) for m in terms of the experimental parameters and variables were sought.

As a starting point the simplest possible boundary conditions were used, namely, complete spin pinning at the boundaries ($m=0$) and stress-free surfaces ($\partial R/\partial z=0$) were assumed. It is conceivable that the actual situation, in regard to appropriate boundary conditions for the film, may be quite complicated near the crossover point because of possible mixing of the simple magnetic and elastic boundary conditions. In the interest of simplicity, however, this complication was not considered.

Solutions which satisfy the boundary conditions are $R=\sum b_k e^{i\omega t}\cos kz$, $m=\sum a_k e^{i\omega t}\sin kz$, and $h=h_0 e^{i\omega t}$ where the a_k and b_k are constant complex amplitudes in the x, y plane, independent of z, and h_0 is the magnitude of the uniform microwave-cavity magnetic field.

ANALYSIS OF DISPERSION

The use of the boundary conditions and the solutions for R, m, and h allow for the solution for a particular a_k in the form $a_k=\chi h_0$, where χ has the role of a complex susceptibility. The real part of χ describes the dispersion of the magnetic waves while the imaginary part of χ describes the absorption of microwave energy by the magnetic system. Reχ vanishes when Imχ becomes maximum. This situation specifies the condition for magnetic resonance, and allows us to solve the expression Re$\chi=0$ for the determined quantity $\Delta\bar{H}_p=[\omega/\gamma-H-(2A/M)k^2]_p$, which is just the magnetic field deviation from the quadratic spin-wave dispersion law for the magnetic resonance corresponding to the pth mode. This definition of $\Delta\bar{H}_p$ differs from the earlier one in that the reference (backgound) dispersion is specified to be quadratic. This is justifiable since the small quartic contribution can be added to the actual dispersion curve to establish the quadratic reference line for each film. Allowing the wave vector to be continuous,

$$\Delta\bar{H}=\frac{b_2^2}{\rho M}\frac{(\omega^2-c_t^2k^2)k^2}{(\omega^2-c_t^2k^2)+(2\omega/\tau_s)^2}, \qquad (5)$$

where the symbols have been defined previously.

Figure 5 shows the result of fitting Eq. (5) to the data of sample 2. Similar results were obtained for sample 1. The agreement is satisfactory near the crossover point, but is less satisfactory far away from that point. The data points return more rapidly to the pure spin-wave dispersion curve than the calculation predicts. The reasons for this are not understood. Certain different combinations of the boundary conditions do not remedy the situation; that is, allowing the spins to be unpinned while the stress does not vanish at the film surfaces or keeping the spins pinned but allowing the surface of the film that is bonded to the substrate to experience stress does not alter Eq. (5). In addition, a more realistic form (allowing for the skin depth) for the microwave magnetic field does not account for the unsatisfactory agreement out on the "wings".

In the last three columns of Table I are to be found the experimentally determined values for c_t, the speed of transverse phonons in the sample material at the microwave frequency, for the magnitude of b_2, the magnetoelastic coupling constant, and for τ_s, the phenomenological phonon relaxation time.

The form of Eq. (5) suggests that the frequency linewidth of $\Delta\bar{H}$ for constant k is simply $\Delta\omega=2\tau_s^{-1}$. Figure 3 may be used to obtain directly $\Delta\omega$ for samples 1 and 2. The τ_s values obtained by this method are identical (within experimental uncertainty) with those obtained by the best fit of Eq. (5) to the data.

The present value for c_t agrees well with reported measurements[6] made at 15 MHz on a bulk sample of permalloy. The determined magnitude of b_2 indicates that it has increased by almost a factor of 2 from room temperature[7] to 77°K. This increase is in agreement with experiments on nickel from 77 to 600°K, in magnetic fields up to 4000 Oe.[8] The temperature dependence of $|b_2|$, along with a slight temperature dependence of τ_s, explains the fact that magnon-phonon coupling was not observed at 298°K. A statement on the acceptability of the values obtained for τ_s must await theoretical and experimental developments concerning the intrinsic nature of τ_s in experiments of this type.

[6] R. Weber, Proc. IEEE **54**, 333 (1966).
[7] J. B. Goodenough and D. O. Smith, Lincoln Laboratory Technical Report No. 197, 1959 (unpublished).
[8] E. Tatsumoto, T. Akamoto, and Y. Kadena, J. Phys. Soc. Japan **20**, 1534 (1965).

Apart from the intrinsic nature of τ_s, one factor to be considered in the experimental determination of the phonon relaxation time is the possible effect of the glass substrate to which one surface of the film is bonded. Such an effect, causing the measured value of τ_s to differ from the intrinsic value, would also affect the value of $|b_2|$ obtained by fitting Eq. (5) to the data.[9]

ANALYSIS OF ABSORPTION

As has been pointed out, the absorption of microwave energy by the sample depends on the magnitude of the imaginary part of the susceptibility. Therefore, it is useful to examine the behavior of $|\mathrm{Im}\chi|$ as a function of the dc magnetic field and as a function of the magnetic wave vector, in order to understand the observed behavior of the resonances. Such an examination shows how the magnetic contributions of the magnetoelastic branches combine to produce a resonance peak. It also explains the important fact that the magnetic field values required for resonance vary in a smooth fashion, with the resonance peaks remaining finite. To facilitate the examination, a starting point is provided by the magnetoelastic dispersion diagram.

Figure 6 shows a typical dispersion diagram for magnetoelastic modes in terms of the spin-wave resonance parameter $\bar{H}$, the magnetic field separation of a point in the spectrum from the $p=0$ uniform mode resonance at constant ω. The dashed, sloping line represents the quadratic spin-wave dispersion in the absence of magnetoelastic coupling, while the dashed horizontal line represents the magnetic-field-independent dispersion curve for transverse phonons in the absence of coupling. The solid curves represent a set of appropriate solutions to the undriven ($h=0$) system of coupled equations of motion. These curves are the branches of the pertinent magnetoelastic modes. With all else constant, an increase in the phonon damping term results in a shift of the magnetoelastic branches towards each other. In fact, for the previously determined values of b_2, c_t, and τ_s, the minimum separation between modes (when wave-vector differences are interpreted in terms of magnetic field) is less than the linewidth of the observed magnetic resonances. Near the crossover point, the linewidths were of the order of 200 Oe, while far from that point the linewidths were of the order of 170 Oe. These facts suggest that as k increases, and the crossover region is traversed, there exists the possibility of a smooth passage (as opposed to a discontinuous "hop" of a resonance peak) from the lower to the upper branch of the magnetoelastic spectrum as a function of magnetic field. There would have been no such possibility of a continuous transition from branch to branch had the phonon damping been small enough and had the magnetic resonance linewidth been narrow enough.

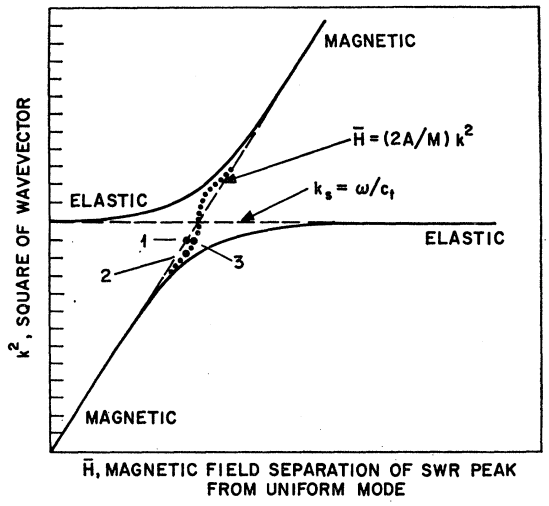

FIG. 6. The theoretical magnon-phonon dispersion diagram as a function of the spin-wave variable $\bar{H}$. The dashed, sloping line represents the dispersion of magnons (quartic term neglected) while the horizontal line represents the dispersion of phonons for the case of zero magnetoelastic coupling. The solid curves represent the magnetoelastic modes which result from the coupling of magnons and phonons for the case of small damping. The dotted curve passing through points 2 and 3 represents the experimentally determined dispersion curve for the observed magnetic resonances in the presence of magnon-phonon coupling.

[9] M. H. Seavey (private communication).

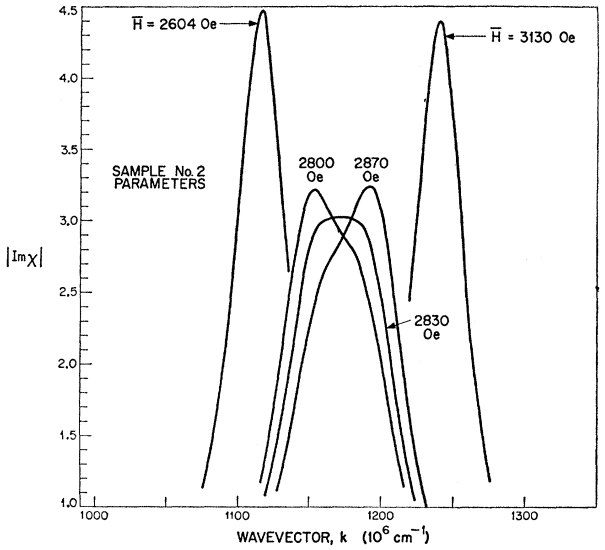

FIG. 7. Computed values of Eq. (6) for $|\mathrm{Im}\chi|$ (in arbitrary units) versus wave vector for sample 2, with $\bar{H}$ as a parameter. The important aspect here is that the absorption by the sample is proportional to $|\mathrm{Im}\chi|$. The crossover frequency of 57.77 GHz was used in the computation. This figure may be used in conjunction with Fig. 6 to explain qualitatively the behavior of the observed resonances as the crossover region is traversed as a function of magnetic field.

The results of a computer calculation of $|\mathrm{Im}\chi|$ versus k, with $\bar{H}$ as a parameter, are shown in Fig. 7. The computation was performed using the parameters of sample 2, with $\mathrm{Im}\chi$ given by

$$\mathrm{Im}\chi = C\,\frac{\phi_s(F+Z\psi+\phi_s\phi_m)-Z(\phi_s\psi-\phi_m Z)}{(F+Z\psi+\phi_s\phi_m)^2+(\phi_s\psi-\phi_m Z)^2}, \quad (6)$$

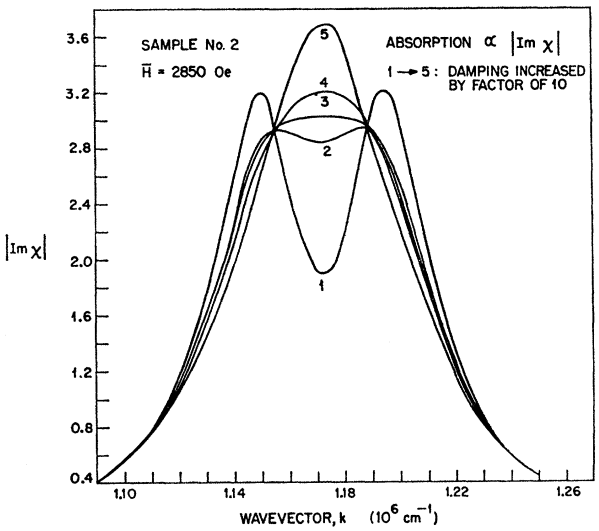

FIG. 8. Computed values of Eq. (6) for $|\mathrm{Im}\chi|$ (in arbitrary units) versus the wave vector for sample 2, with the phonon damping (proportional to τ_s^{-1}) as a parameter. The values for the microwave frequency and $\bar{H}$ correspond to the crossover values. The behavior of these peaks can be understood, in conjunction with Fig. 6, by noting: (a) The linewidths of the observed resonances were quite large, and (b) as phonon damping increases, the separation between the magnetoelastic branches decreases.

where C includes factors which are functions of the mode number of the resonance peak, the geometry of the experiment, the uniformity of the rf magnetic field in the film, the saturation magnetization of the film, and the assumed boundary conditions. In Eq. (6), $\phi_s=(2c_t^2/\omega\tau_s)k^2$, $F=(\gamma b_2^2/\rho M_s)k^2$, $\phi_m=1/\tau_m$, $Z=(\omega^2-c_t^2k^2)$, and $\psi=[(2A/M_s)\gamma k^2-\gamma\bar{H}]$.

A fixed value of $\bar{H}$ can be visualized as a vertical line on the dispersion diagram of Fig. 6. As k is increased from zero, it is to be expected that $|\mathrm{Im}\chi|$ will pass through a maximum for each pair $(k,\bar{H})$ that falls on one of the magnetoelastic modes. The amplitude of the maximum depends on the magnetic wave content of that particular mode. In Fig. 7, the $\bar{H}=2604$- and 3130-Oe curves represent resonances due to the lower and the upper branches of the magnetoelastic spectrum, respectively. Contributions from the opposite branches (i.e., the predominantly elastic branches) were not revealed in the calculations for these cases, indicative of the extremely small magnetic content of these branches far removed from the crossover region. A single resonance peak is also obtained for the crossover value of $\bar{H}=2830$ Oe. Its broadness is, however, suggestive of strong overlap of the magnetic contributions from the separate magnetoelastic branches of the spectrum. The shapes of the absorption curves for the remaining cases (i.e., for $\bar{H}=2800$ and 2870 Oe), are clear examples of the combining of separate magnetic contributions from the individual branches. These curves, close to the crossover point, may be used in conjunction with Fig. 6 to gain additional insight into the experimentally observed behavior of the resonance peaks. As an example of their use, let us suppose that point 1 of Fig. 6 locates a peak in the absence of magnon-phonon coupling. This point determines specific values of k and $\bar{H}$. If the coupling were now "turned on", the peak of the combined absorption curve would occur at a lower k value than the specified value. This is evident from the shape of the appropriate $H=2800$-Oe curve of Fig. 7. This shift of the resultant peak arises from the fact that the magnetic contribution of the lower branch is greater than that of the upper branch on this side of the crossover point. Point 2 on Fig. 6 corresponds to the reduced value of k and the original value of $\bar{H}$. To retune for resonance at the originally specified, allowed k value, $\bar{H}$ must be increased until point 3 is reached. Continuation of this process for additional resonances in the crossover region leads to a complete qualitative description of the data.

The curves of Fig. 8 show the response of the resonance peak at the crossover point to changes in the phonon damping ($\propto\tau_s^{-1}$). The parameters of sample 2, including the measured value of τ_m, were used in the computation. The curve corresponding to $\tau_s=0.93\times10^{-10}$ sec, the value determined by fitting Eq. (5) to the data, lies between the curves marked 4 and 5. It is to be noted that even for the extremely small phonon damping used to compute curve 1, $|\mathrm{Im}\chi|$ does not vanish at crossover because the linewidths of the magnetic resonances are greater than the separation between the branches of the magnetoelastic spectrum.

ACKNOWLEDGMENTS

Thanks are due to the members of H. J. Zeiger's Solid State Theory Group for valuable discussions. The continued support during the course of this work and the careful readings of the final manuscript by P. E. Tannenwald and J. G. Mavroides are appreciated. The technical assistance of J. W. Burke, the computer programming of B. Palm and S. Landon, and the competent library research of J. Katayama are gratefully acknowledged.